

1 **Production, characterization, and epitope mapping of a**
2 **monoclonal antibody against genotype VII Newcastle**
3 **disease virus V protein**

4
5 **Li J¹, Meng C¹, Ren T¹, Wang W¹, Zhang Y¹, Yuan W¹, Xu S¹, Sun Y¹, Tan**
6 **L¹, Song C¹, Liao Y¹, Nair V², Munir M², Ding Z³, Liu X⁴, Qiu X⁵, Ding C⁶**

7
8
9 *1 Shanghai Veterinary Research Institute, Chinese Academy of Agricultural*
10 *Sciences, Shanghai 200241, PR China.*

11 *2 The Pirbright Institute, United Kingdom.*

12 *3 Laboratory of Infectious Diseases, College of Veterinary Medicine, Jilin University,*
13 *Changchun 130062, PR China.*

14 *4 Key Laboratory of Animal Infectious Diseases, Yangzhou University, Yangzhou*
15 *225009, PR China; Jiangsu Co-innovation Center for Prevention and Control of*
16 *Important Animal Infectious Diseases and Zoonoses, Yangzhou 225009, PR China.*

17 *5 Shanghai Veterinary Research Institute, Chinese Academy of Agricultural*
18 *Sciences, Shanghai 200241, PR China. Electronic address: xsqiu1981@shvri.ac.cn.*

19 *6 Shanghai Veterinary Research Institute, Chinese Academy of Agricultural*
20 *Sciences, Shanghai 200241, PR China; Jiangsu Co-innovation Center for Prevention*
21 *and Control of Important Animal Infectious Diseases and Zoonoses, Yangzhou*
22 *225009, PR China.*

23
24 **Electronic address:** shoveldeen@shvri.ac.cn.
25
26
27
28
29
30
31
32
33
34
35
36
37
38
39
40
41
42
43
44
45
46
47
48
49

50 **Abstract**

51

52 Newcastle disease virus (NDV) V protein is crucial for viral interferon (IFN)
53 antagonism and virulence, determining its host range restriction. However, little
54 information is available on the B cell epitopes of V protein and the subcellular
55 movement of V protein in the process of NDV infection. In this study, the monoclonal
56 antibody (mAb) clone 3D7 against genotype VII NDV V protein was generated by
57 immunizing mice with a purified recombinant His-tagged carboxyl-terminal domain
58 (CTD) region of V protein. Fine epitope mapping analysis and B-cell epitope
59 prediction indicated that mAb 3D7 recognized a linear epitope ¹⁵²RGPAELWK¹⁵⁹,
60 which is located in the V protein CTD region. Sequence alignment showed that the
61 mAb clone 3D7-recognized epitope is highly conserved among Class II genotype VII
62 NDV strains, but not among other genotypes, suggesting it could serve as a genetic
63 marker to differentiate NDV genotypes. Furthermore, the movement of V protein
64 during NDV replication in infected cells were determined by using this mAb. It was
65 found that V protein localized around the nucleus during virus replication. The
66 establishment of V protein-specific mAb and identification of its epitope extend our
67 understanding of the antigenic characteristics of V protein and provide a basis for the
68 development of epitope-based diagnostic assays.

69

70 **1. Introduction**

71 Newcastle disease (ND) is one of the most serious infectious diseases of birds
72 causing major economic losses to the poultry industry (Aldous and Alexander, 2001;
73 Dimitrov et al., 2016). Its causative agent, virulent Newcastle disease virus (NDV),
74 belongs to the genus Avulavirus, in the subfamily Paramyxovirinae, family
75 Paramyxoviridae, order Mononegavirales (de Leeuw and Peeters, 1999).
76 Phylogenetically, NDVs have been classified into two major categories, class I and
77 class II (Czegledi et al., 2006; Gould et al., 2003). Class I NDVs are occasionally
78 isolated from wild aquatic birds and domestic poultry and all but one are nonvirulent
79 (Liu et al., 2009; Mia Kim et al., 2007). Class II NDVs, which were recently
80 subcategorized into 18 genotypes, are genetically and phenotypically more diverse,
81 and exhibit a wider range of virulence (Diel et al., 2012; Dimitrov et al., 2016; Miller
82 et al., 2010; Ramey et al., 2013).

83

84 NDV has a negative-sense, single-stranded continuous RNA genome of 15,186,
85 15,192 or 15,198 nucleotides (nt) that contains six genes in the order 3'-NP-P-M-F-
86 HN-L-5', encoding the six viral proteins nucleoprotein, phosphoprotein, matrix
87 protein, fusion protein, hemagglutinin-neuraminidase and large protein (Yusoff and
88 Tan, 2001). Two additional proteins, V and W, are encoded by mRNAs derived from
89 the P gene via RNA editing (Qiu et al., 2016a; Steward et al., 1993). In the process
90 of P gene transcription, some transcripts have inserts of one or more pseudo-
91 template G nucleotides behind the RNA-editing site, leading to open reading frame
92 (ORF) frameshift. The reported proportions of protein-encoding mRNAs in NDV-
93 infected cells are about 68% for P, 29% for V, and 2% for W (Mebatsion et al., 2001;
94 Qiu et al., 2016a). P, V and W protein shared a common N-terminal moiety of ORF
95 and contained unique C-terminal moiety (Huang et al., 2003; Park et al., 2003a).

96

97 The V protein of paramyxoviruses is characterized by a unique cysteine-rich
98 carboxyl-terminal domain (CTD), which binds two zinc atoms (Paterson et al., 1995;
99 Steward et al., 1995) and is important for viral interferon (IFN) antagonism in a

100 variety of ways (Horvath, 2004b). The V protein of parainfluenza virus 5 (PIV5) and
101 mumps virus (MuV) target signal transducer and activator of transcription 1 (STAT1)
102 for proteasome-mediated degradation through assembly of a degradation complex
103 containing signal transducer and activator of transcription 2 (STAT2), damaged DNA
104 binding protein 1, and cullin 4 A (Didcock et al., 1999; Kubota et al., 2001). The V
105 proteins of Nipah virus and Hendra virus inhibit cellular responses to IFN through
106 binding and cytoplasmic sequestration of both STAT1 and STAT2 (Rodriguez et al.,
107 2002, 2003). Measles virus (MV) V protein inhibits host IFN-induced transcriptional
108 responses by preventing IFN-induced STAT1 and STAT2 nuclear import (Palosaari
109 et al., 2003).

110
111 Similar to PIV5, NDV V protein is a structural component of virions and considered
112 an effector for IFN antagonism (Paterson et al., 1995; Steward et al., 1995);
113 however, its underlying mechanism is unknown. Based on reverse genetics, several
114 V-deficient NDV mutants have been recovered, which were much more sensitive to
115 the antiviral effects of IFN (Alamares et al., 2010; Mebatsion et al., 2001; Park et al.,
116 2003a; Qiu et al., 2016b); resistance to IFN is restored when V protein is re-
117 expressed in infected cells (Park et al., 2003a). NDV inhibits IFN through the C-
118 terminal region of the V protein, which promotes degradation of phosphorylated
119 STAT1 and blocks IFN signaling (Huang et al., 2003; Park et al., 2003b; Qiu et al.,
120 2016b).

121
122 Due to lack of commercial antibodies against V protein, little is known about
123 structural and antigenic differences of V protein between different NDV strains, nor
124 the detailed IFN antagonism mechanism of NDV V protein. In this study, a
125 recombinant protein containing the CTD domain of NDV V protein was used as an
126 antigen for production of mouse hybridomas that secreted an anti-V protein
127 monoclonal antibody (mAb). Sensitivity and specificity of the anti-V mAb was
128 examined by enzyme-linked immunosorbent assay (ELISA), Western blot (WB) and
129 indirect immunofluorescence assay (IFA). The epitope recognized by the mAb were
130 also identified by WB and ELISA assay. Our study indicated that the mAb we
131 developed could be a useful tool for investigating the antigenic structure and function
132 of NDV V protein.

133

134 **2. Materials and methods**

135 **2.1. Virus, cells and plasmids**

136 NDV strains used in this study, La Sota/46, Mukteswar, Queensland V4, Herts/33,
137 F48E8 and Hitchner B1, were from China Institute of Veterinary Drug Control.
138 Pi/China/SD/2012/132 (designated ND132 in this study), Pi/China/SD/2012/167
139 (ND167), CN/ZJ-1/00 (ZJ-1), JSD0812 and JS-7-05-Ch (HM) were previously
140 isolated on mainland China (Dai et al., 2014; Qiu et al., 2011). All viruses were
141 maintained in our laboratory (Detailed information on NDV strains is in Table 1). All
142 viruses were propagated in 9- to 11-day-old specific-pathogen-free chicken
143 embryonated eggs as previously described (Gough et al., 1988). Fresh allantoic fluid
144 was harvested from embryonated eggs dead between 24 and 120 h after inoculation
145 and kept at -80 °C. DF-1, HeLa and SP2/0 cells were from the American Type
146 Culture Collection and cultured in Dulbecco's modified Eagle's medium (DMEM;
147 Gibco, Grand Island, NY) or RPMI 1640 medium (Gibco) containing 10% fetal bovine
148 serum (FBS, Gibco) at 37 °C and 5% CO₂. Prokaryotic expression plasmid pET-28a-
149 ZJ1/VCD encoding the C-terminal domain of ZJ1 and eukaryotic expression plasmid

150 pFLAG-ZJ1-V encoding the complete V protein of ZJ1 were constructed previously
151 (Qiu et al., 2016b).

152

153 **2.2. Expression and purification of recombinant protein**

154 The His-tagged CTD region of V protein (VCD) from strain ZJ1 was prepared,
155 purified and quantified according to previous reports (Qiu et al., 2016b). The pET-
156 28a-ZJ1/VCD was transformed into Escherichia coli. (E. coli.) BL21 and induced at
157 37 °C for 8 h with 1 mM isopropyl-β-D-thiogalactoside. Bacteria were harvested by
158 centrifugation at 5000g and washed for three times in phosphate buffered saline
159 (PBS). Pellets were resuspended in buffer A (50 mM Tris-HCl pH 8.0, 300 mM NaCl,
160 20 mM imidazole, 1 mM phenylmethylsulfonyl fluoride) supplemented with lysozyme
161 (0.4 mg/mL) and DNase I (10 µg/mL). After 30 min with gentle shaking, bacteria were
162 sonicated on ice. After centrifugation at 13,000 g for 20 min at 4 °C, pellets were
163 collected and solubilized overnight with gentle shaking at 4 °C in 50 mM Tris-HCl (pH
164 8.0) containing 8 M urea, 0.5 M NaCl, 5 mM 2-mercaptoethanol and 5 mM imidazole.
165 Supernatant containing solubilized inclusion bodies was collected after centrifugation
166 at 12,000 g for 15 min. Purified recombinant protein was harvested from
167 supernatants using Ni-NTA His•Bind Resin (Novagen, Madison, WI, USA) according
168 to the manufacturer's instruction. Recombinant His-tagged VCD (His-VCD) protein
169 was confirmed by sodium dodecyl sulfate polyacrylamide gel electrophoresis (SDS-
170 PAGE) and WB with anti-His (Sigma-Aldrich, St. Louis, MO). Protein concentration
171 was determined using Bio-Rad protein assay reagent (Bio-Rad, Hercules, CA).

172

173 **2.3. Immunization of mice and establishment of hybridomas**

174 Six-week-old female BALB/c mice (SPF grade) were purchased from the Shanghai
175 SLAC Laboratory Animal Co., Ltd. (China). The His-VCD protein was emulsified with
176 an equal amount of Freund's complete adjuvant (Sigma-Aldrich, USA) and
177 subcutaneously immunized the mice in the abdomen with 50 µg His-VCD protein for
178 each mouse. Four weeks after priming, mice were boosted four times in 2-week
179 intervals by intraperitoneal injection of 100 µg His-VCD protein per mouse. Five days
180 after last injection, spleen cells were collected from immunized mice, washed twice
181 with RPMI 1640 medium, and mixed and fused with logarithmically growing SP2/0
182 myeloma cells in a ratio of 5:1 in the presence of polyethylene glycol 4000 (Sigma-
183 Aldrich, St. Louis, MO, USA). Treated cells were suspended in HAT (RPMI 1640
184 medium containing 20% FBS, 100 mg/mL streptomycin, 100 IU/mL penicillin,
185 100 mM hypoxanthine, 16 mM thymidine, and 400 mM aminopterin), and plated into
186 96-well tissue culture plates at 1×10^5 cells per well in 200 µL media. After
187 cultivation at 37 °C at 5% CO₂ for 10 days, medium was detected for anti-VCD
188 antibodies by indirect ELISA with His-VCD protein. Positive hybridoma cells were
189 subcloned though a limited dilution method several times until monoclonal hybridoma
190 cells were established following standard procedures. Hybridoma cells were cultured
191 in the abdominal cavity of liquid-paraffin-primed BALB/c mice to obtain ascitic fluid.
192 Globulin fractions were precipitated with 2 M (NH₄)₂SO₄ and purified by gel filtration
193 with Sephacryl S-200 HR (GE Healthcare UK Ltd.). MAbs clones were tested for
194 immunoglobulin class/subclass using the SBA Clonotyping System
195 (SouthernBiotech, USA).

196

197 **2.4. Indirect enzyme-linked immunosorbent assays**

198 Purified ZJ1-VCD protein or fresh allantoic fluid for distinct NDV strains treated with
199 an equal amount of 0.1% SDS at 100 °C for 10 min were used as detection antigens.

200 Microtiter ELISA plates with 96 wells were coated with 1:200 dilutions of prepared
201 allantoic fluid or 1 ng/ μ L purified ZJ1-VCD protein in 100 μ L carbonate buffer solution
202 (CBS) per well. After cultivation at 4 °C overnight, ELISA plates were washed three
203 times with PBS containing 0.05% Tween-20 (PBST) and blocked with 300 μ L/well
204 5% skim milk powder in PBST for 2 h at 37 °C. Hybridoma cultured medium or
205 antibodies were plated into coated ELISA plates, 100 μ L per well, and incubated at
206 37 °C for 1 h. After washing three times with PBST, plates were incubated with
207 1:6000 diluted horseradish peroxidase-conjugated goat anti-mouse IgG (Santa Cruz,
208 CA, USA) for 1 h at 37 °C. To each well, 100 μ L 3,3',5,5'-tetramethylbenzidine
209 (Sigma-Aldrich, USA) was added and absorbance was measured at 450 nm in a
210 microplate reader (Synergy 2, BioTek).

211

212 **2.5. Specificity of mAbs for NDV genotypes**

213 DF-1 cells were cultured in 6-well plates, washed 3 times with PBS, and incubated
214 with NDV strains at multiplicity of infection (MOI) 5 in 600 μ L DMEM per well at 37 °C
215 for 30 min. Supernatants were discarded and cells cultured in DMEM containing 2%
216 FBS (Gibco). At indicated time points, cells were washed thoroughly and subjected
217 to IFA and WB assays with anti-VCD mAbs.

218

219 **2.6. Western blots**

220 Cells harvested at indicated time points were washed three times with PBS and
221 lysed with RIPA buffer (50 mM Tris-HCl pH 7.6, 150 mM NaCl, 1% v/v NP-40, 1%
222 w/v sodium deoxycholate, 0.1% w/v sodium dodecyl sulfate, 1 mM
223 phenylmethanesulfonyl fluoride, 1 mM Na₃VO₄, 1 mM NaF, 0.15 μ M aprotinin, 1 μ M
224 leupeptin, and 1 μ M pepstatin). Lysates were incubated at 100 °C for 10 min after
225 addition of 5x SDS-PAGE loading buffer (250 mM Tris-HCl, pH 6.8, 10% SDS, 0.5%
226 bromophenol blue, 50% glycerol, 5% β -mercaptoethanol), and proteins separated by
227 SDS-PAGE on 10% polyacrylamide gels before transferring to nitrocellulose
228 membranes (Millipore, Billerica, MA, USA). Membranes were blocked overnight at
229 4 °C in Tris-HCl buffer solution (TBS) containing 5% skim milk, then for 2 h with anti-
230 VCD mAb, anti-NP mAb(Zhan et al., 2014) or anti-FLAG (positive control). After
231 incubation with 1:6000 diluted HRP-goat anti-mouse IgG (Santa Cruz) in TBS for 1 h
232 at room temperature, blots were visualized using an enhanced chemiluminescence
233 detection system (Thermo Fisher Scientific, Waltham, MA, USA).

234

235 **2.7. Indirect immunofluorescence assays**

236 MAbs were detected in IFA according to previously described procedures (Sun et al.,
237 2017). DF1 cells cultured on glass coverslips were infected with ZJ1 virus at a MOI
238 of 5. Cells were fixed with 4% formaldehyde solution for 10 min at 6, 8, 10, 12, 18,
239 and 24 h post infection (hpi), and permeabilized with 0.25% Triton X-100 for 10 min
240 at ambient temperature. After blocking with PBS containing 3% bovine serum
241 albumin (BSA), cells were incubated with mAb for 1 h at 37 °C. Unbound antibodies
242 were removed with PBST three times and cells were incubated with anti-mouse IgG
243 Alexa Fluor 488 (Zymed-Invitrogen, CA, USA) for 1 h. After staining with 4',6-
244 diamidino-2-phenylindole (DAPI) for 10 min, coverslips were examined using a Zeiss
245 Laser confocal fluorescence microscope (Nikon, JPN).

246

247 **2.8. Plasmid construction for epitope mapping**

248 To map the epitopes of generated mAbs, a series of eukaryotic plasmids expressing
249 truncated V proteins were constructed. Consecutive truncations were introduced to

250 the V protein ORF of pFLAG-ZJ1-V by overlapping PCR using PfuUltra II Fusion HS
251 DNA polymerase (Stratagene, Agilent, US). Primers and locations of truncated
252 sequences are in Table 2, Table 3. PCR was 30 cycles of 98 °C 10 s, 58 °C 20 s and
253 72 °C 8 min. After purification by PCR purification kits (Axygen), PCR products were
254 digested with DpnI (Fermentas) at 1 U/μL at 37 °C for 1 h with inactivation at 80 °C
255 for 10 min. Digested PCR products were directly transformed into *E. coli* DH5α. All
256 plasmids were identified by sequencing (Sangon Biotechnology, Shanghai, China).

257

258 **2.9. Plasmid transfection**

259 HeLa cells at 70% confluence, seeded in 6-well plates, were transfected with
260 pFLAG-ZJ1-V and derived recombinant plasmids using FuGENE HD transfection
261 reagent (Promega, Madison, WI, USA) according to the manufacturer's instructions.
262 Transfected cells were harvested at 48 h post transfection and subjected to FLAG-
263 tagged V protein detection by WB.

264

265 **2.10. Polypeptide design and detection**

266 To fine-map epitopes recognized by mAb 3D7, three polypeptides spanning amino
267 acid (aa) 144–167 of V protein were synthesized by GL Biochem (Shanghai, China)
268 were 144SPTSGPTTRGPAELWK159, 147SGPTTRGPAELWKQPGK163 and
269 152RGPAELWKQPGKTAAS167. A panel of polypeptide mutants was synthesized
270 based on 147SGPTTRGPAELWKQPGK163, in which certain aa residues were
271 replaced by alanine (A) and named S147 A, G148 A, P149 A, T150 A, T151 A,
272 R152 A, G153 A, P154 A, E156 A, L157 A, W158 A, K159 A and Q160 A. Purified
273 His-VCD was the positive control and an irrelevant peptide (aa 40PQGKTKALSTA50
274 from ZJ1 V protein) was the negative control. Reactivity of mAb 3D7 with each
275 polypeptide was determined by ELISA and WB.

276

277 **2.11. Bioinformatics analysis**

278 Prediction of aa sequences, alignment of sequences and phylogenetic analysis used
279 the MegAlign program in the Lasergene package (DNASTAR Inc., Madison, WI,
280 USA). V protein sequences of 27 reference NDV strains of different genotypes were
281 from EMBL/GenBank (Table 1). BepiPred-2.0 online software was used to predict
282 sequential B-cell epitopes of NDV V protein
283 (<http://www.cbs.dtu.dk/services/BepiPred/>). Amino acid sequences of NDV V
284 proteins were sent to Swiss Model (<http://swissmodel.expasy.org/>) for modelling of a
285 three-dimensional (3D) structure of NDV V protein, which was subjected to
286 DiscoTope 2.0 Server for discontinuous B-cell epitope analysis (Kringelum et al.,
287 2012).

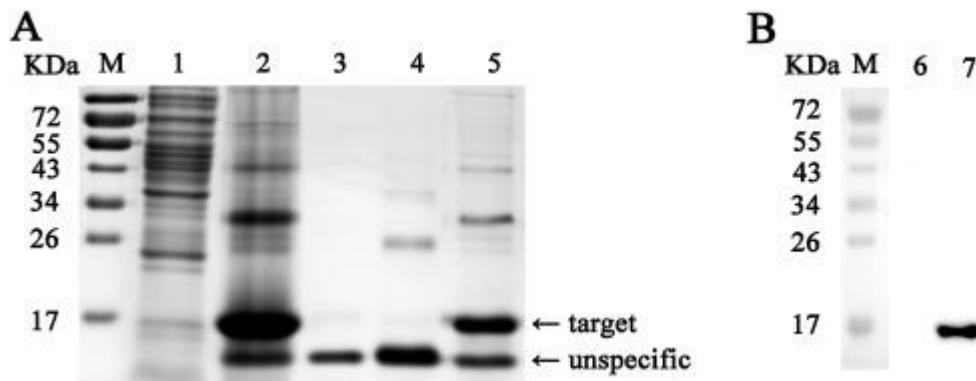
288

289 **3. Results**

290 **3.1. Expression and purification of recombinant NDV ZJ1-VCD protein**

291 A His-tagged form of NDV V protein CTD polypeptide was highly expressed by pET-
292 28a-ZJ1/VCD in *E. coli* and had a molecular weight of 15 kDa as determined by
293 SDS-PAGE, as predicted (Fig. 1A). Recombinant protein His-VCD was purified
294 through Ni-chelating affinity chromatography under denaturing conditions and
295 confirmed by WB with anti-His, in which a single band with the expected molecular
296 weight of approximately 15 kDa was observed (Fig. 1B). The recombinant protein
297 was harvested and used as the antigen for immunization and detection.

298



299
300

301 *Fig. 1. SDS-PAGE and Western blot assays for the recombinant CTD polypeptide of*
 302 *NDV V protein expressed from pET-28a-ZJ1/VCD in E. coli BL21. (A) SDS-PAGE*
 303 *assay of His-tagged form of the ZJ1 V protein CTD region expressed in E. coli. (B)*
 304 *WB assay of the purified recombinant protein His-VCD using anti-His. M, PageRuler*
 305 *prestained protein ladder; 1 and 6, E. coli BL21 lysate (negative control); 2, total His-*
 306 *VCD expressed from pET28a-VCD; 3, His-VCD expressed in the supernatant; 4 and*
 307 *7, His-VCD expressed in inclusion bodies; 5, His-VCD purified from inclusion bodies.*

308

309 **3.2. Generation of the mAb 3D7 against NDV V protein**

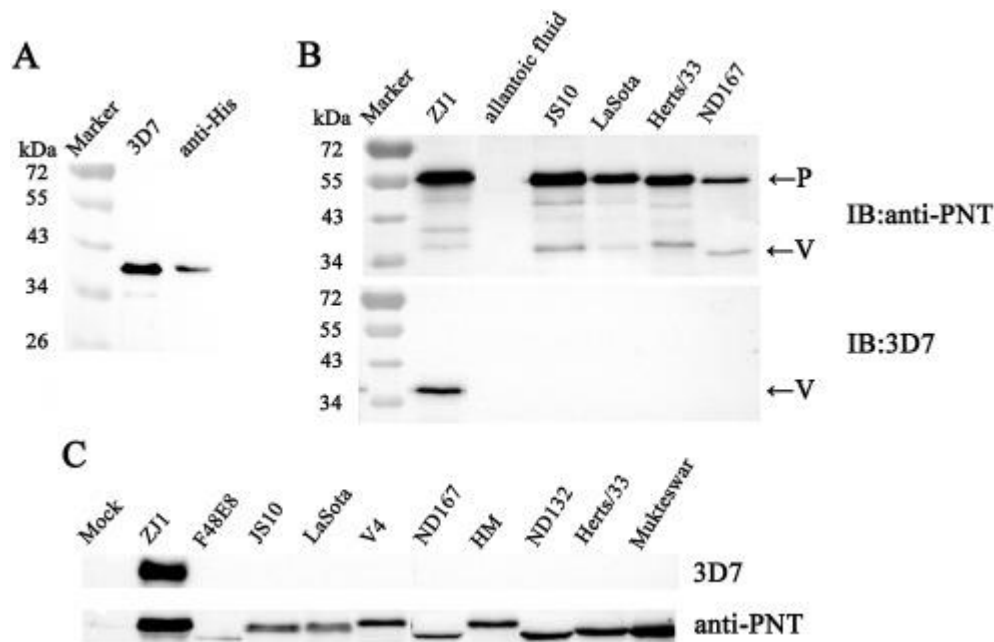
310 Five hybridoma cell lines were acquired and only one stably produced antibodies
 311 that reacted strongly with His-VCD in indirect ELISA and IFA (data not shown). This
 312 mAb clone was designated as 3D7. Using a commercially available isotyping kit
 313 (Roche), the mAb 3D7 heavy chain was determined to be IgG1 and the light chain
 314 was κ . The ascites fluid of mAb 3D7 was produced and purified to the final
 315 concentration of 1.5 mg/mL.

316

317 **3.3. Specificity of the mAb 3D7 for different NDV genotypes**

318 As shown in Fig. 2A, the mAb 3D7 reacted with the recombinant His-tagged V
 319 protein expressed by pFLAG-ZJ1-V in DF1 cells. A single band of about 35 kDa was
 320 observed, the same as the result with anti-His antibodies. Further, the purified ZJ-1
 321 (class II, genotype VII), JS10 (class I), La Sota/46 (class II, genotype II), Herts/33
 322 (class II, genotype IV) and ND167 (class II, genotype VI) viruses were detected in
 323 WB to determine the reactivity of mAb 3D7 with distinct NDV virions. Both P and V
 324 protein were detectible in all of the NDV virions using antiserum anti-PNT; however,
 325 mAb 3D7 reacted only with the V protein of ZJ1, but not any other strains.

326



327
328

329 *Fig. 2. Reactivity and specificity assay of mAb clone 3D7 by Western blot. (A) WB*
330 *assay of the His-tagged V proteins expressed by the recombinant plasmid pFLAG -*
331 *ZJ1-V in DF1 cells using anti-His or mAb 3D7 antibodies. (B) WB assay of V and P*
332 *proteins contained in different NDV virions using the mAb 3D7 and antiserum anti-*
333 *PNT. (C) WB assays of the V and P protein expressed in NDV-infected DF1 cells.*

334

335 This result was confirmed in NDV-infected DF1 cells. Using mAb 3D7, V protein with
336 a molecular weight of 35 kDa was detected only in ZJ1-infected DF1 cells (Fig. 2C),
337 but not any other NDV-infected cells, involving JS10 (class I), V4 (class II, genotype
338 I), La Sota/46 (class II, genotype II), Mukteswar, HM (class II, genotype III), Herts/33
339 (class II, genotype IV), ND132, ND167 (class II, genotype VI) and F48E8 (class II,
340 genotype IX). As a comparison, P protein were detected in those NDV strains-
341 infected cells, with varying molecular weights of around 55 kDa. This result was
342 probably due to different phosphorylation levels of P protein in different strains (Qiu
343 et al., 2016c).

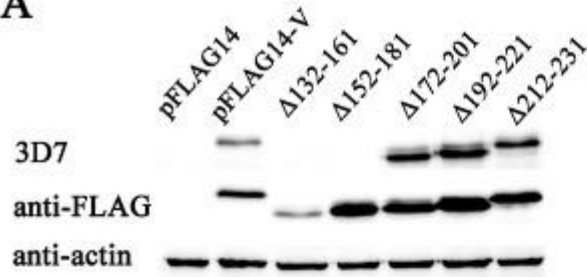
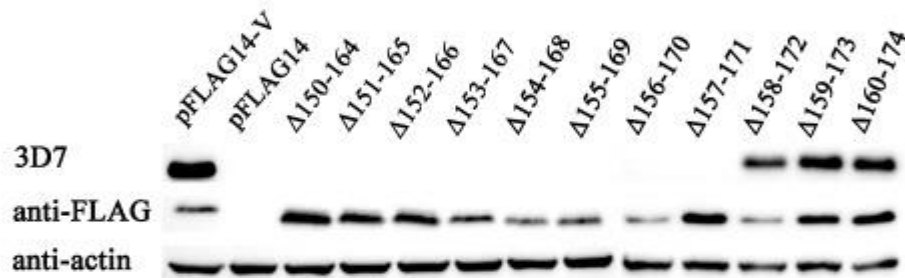
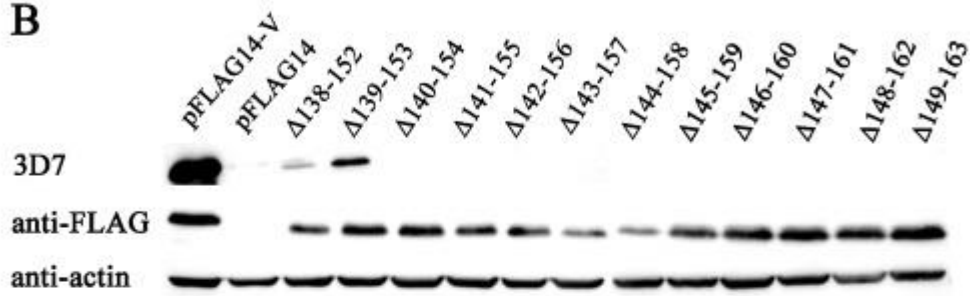
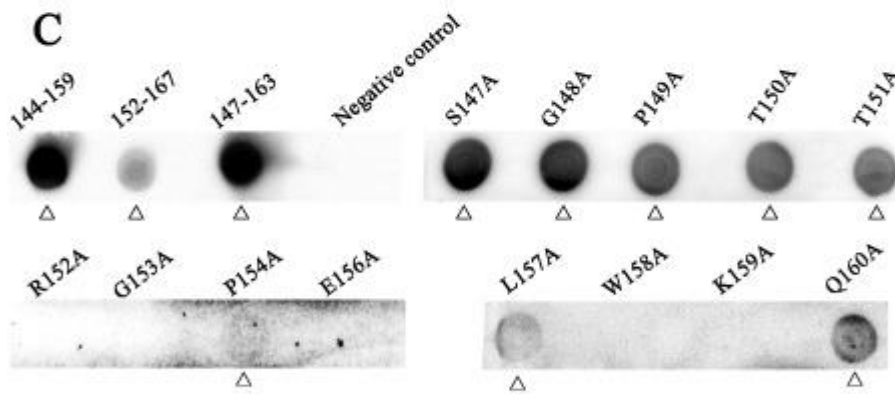
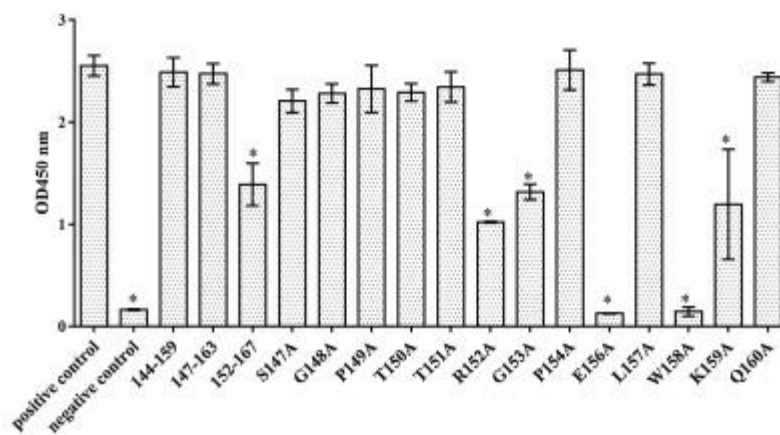
344

345 Indirect ELISA assay was performed and the titer of mAb 3D7 against purified His-
346 VCD protein was 1:3200. The mAb 3D7 never react with all the virus detected except
347 for ZJ1. The titer was 1:800.

348

349 **3.4. Identification of B cell epitopes recognized by the mAb 3D7**

350 The epitopes recognized by mAb 3D7 was mapped in WBs with NDV V protein and
351 its derived protein mutants. As shown in Fig. 3A, the mAb 3D7 did not react with V
352 protein when aa 132-161 or 152-181 were truncated; by contrast, the truncation of
353 172-201, 192-221, 212-231 from V protein never influenced the reactivity of 3D7.
354 Subsequent experiments showed that truncated V protein mutants without peptides
355 spanning aa 140-154, 141-155, 142-156, 143-157, 144-158, 145-159, 146-160, 147-
356 161, 148-162, 149-163, 150-164, 151-165, 152-166, 153-167, 154-168, 155-169,
357 156-170 or 157-171 were not recognized by mAb 3D7 (Table 3 and Fig. 3B). These
358 peptides contain 154PAEL157 as the common aa, suggesting that mAb 3D7
359 recognized epitope was between aa 140 and 171 and peptide 154PAEL157 was
360 essential.

A**B****C****D**

363

364 *Fig. 3. Mapping of the epitope recognized by mAb 3D7. (A) WB detection of a panel*
365 *of recombinant V protein, in which 30 aa were consecutively truncated in the CTD*
366 *region. All the V protein mutants and their deleted regions are listed in Table 2. (B)*
367 *WB detection of a panel of recombinant V protein, in which 15 aa were consecutively*
368 *truncated in the ORF spanning from aa 138 to 174. All the V protein mutants and*
369 *their deleted regions are listed in Table 3. (C) Dot blots detection for the mAb 3D7*
370 *using synthesized peptides. The labels 144-159, 147-163 and 152-167 indicate the*
371 *peptides 144SPTSGPTTRGPAELWK159, 147SGPTTRGPAELWKQPGK163 and*
372 *152RGPAELWKQPGKTAAS167, respectively. S147 A, G148 A, P149 A, T150 A,*
373 *T151 A, R152 A, G153 A, P154 A, E156 A, L157 A, W158 A, K159 A and Q160 A*
374 *indicate the polypeptide mutants based on 147SGPTTRGPAELWKQPGK163, in*
375 *which certain aa was replaced by alanine. All the positive results are labeled with Δ*
376 *under the blot. (D) Dot ELISA detection for the mAb 3D7 using synthesized peptides.*
377 *Error bars represent standard deviation. The OD450 value of synthesized peptides*
378 *were compared with the positive control by using the Student's t-test and the ELISA*
379 *readings that were significantly different from the positive control are labelled **
380 *($P < 0.05$).*

381

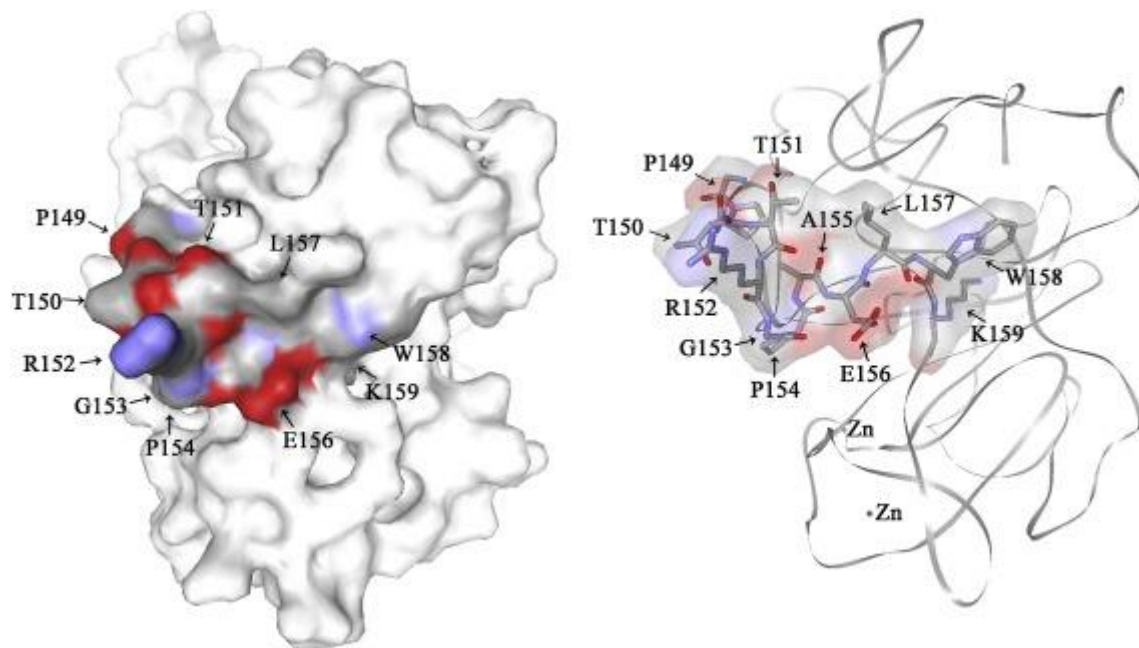
382 Fine mapping of the epitope was performed by dot blots and dot ELISAs using three
383 synthesized peptides spanning aa 144-159, 147-163 and 152-167 of V protein.
384 Reactivity of 3D7 with peptide 152-167 in dot blots was impaired compared to
385 peptides 144-159 and 147-163 (Fig. 3C). In dot ELISAs, all three peptides were
386 recognized by 3D7. The OD450 of peptide 152-167 was slightly lower than other
387 peptides (Fig. 3D). This result suggested that aa region 147-159 was involved in
388 formation of the epitope, but only the common aa sequence 152RGPAELWK159 of
389 these peptides was essential. A panel of point mutations was introduced into the
390 synthesized peptides. Removal of residues at R152, G153, E156, W158 and K159
391 blocked recognition by 3D7 in dot blots; while the residue removal at S147, G148,
392 P149, T150 and T151 did not influence the reactivity with 3D7. Besides, the mutation
393 of P154 and L157 compromised mAb reactivity. Similar results were observed in dot
394 ELISA results, the ELISA readings of 3D7 with the peptide mutant R152 A, G153 A,
395 E156 A, W158 A and K159 A were significantly lower than the positive control. In
396 addition, residue K159 was not recognized by the mAb in dot blot assays but was
397 detectable in dot ELISA assays (Fig. 3C and D).

398

399 **3.5. Protein modelling and B-cell epitope analysis of NDV V protein**

400 The complete 3D structure of the NDV V protein was modelled according to the
401 crystal structure of its counterpart of PIV5 (Fig. 4). The 3D7-recognized epitope was
402 in the region spanning aa 140–171, all of which was exposed on the surface of V
403 protein. The region 147-159, determined to be recognized by 3D7 were marked in
404 the 3D structure of V protein. The V protein structure displayed that the crucial
405 peptide 154PAEL157 of the 3D7 recognized epitope was not in a same plane with aa
406 147-151, suggesting that aa 147-151 was not a crucial element for direct mAb
407 binding. The linear B-cell epitopes of the NDV V protein was predicted from the
408 primary protein sequences and the discontinuous B-cell epitopes was predicted
409 based on the 3D structure, all of which covered the identified 3D7-recognized
410 peptide 152RGPAELWK159 (Table 4).

411



412
413

414 *Fig. 4. Relative localization of the identified epitopes in the predicted 3D structure of*
 415 *the NDV V protein. The three-dimensional structure of the NDV V protein was*
 416 *modelled by the online services Swiss Model. The identified mAb 3D7-recognized*
 417 *peptide ¹⁵²RGPAELWK¹⁵⁹ and its structurally supporting part is labeled blue and red*
 418 *in the figure. The red areas represent oxygen and the blue areas indicate nitrogen.*
 419 *The model on the left is the predicted V protein structure with the calculated surface*
 420 *structure; while the model on the right displays the atoms of the mAb 3D7-*
 421 *recognized peptide in a NDV V protein backbone without showing the surface*
 422 *structure. (For interpretation of the references to colour in this figure legend, the*
 423 *reader is referred to the web version of this article.)*

424

425 **3.6. Specificity and conservation of the epitope among NDV strains**

426 V proteins from distinct NDV genotypes (Table1) were aligned for analysis. The mAb
 427 clone 3D7-recognized epitope 147SGPTTRGPAELWK159 and its surrounding
 428 region aa 140–146 and 160–171 were conserved among genotype VII NDV strains;
 429 however, the epitope shared low identity among other genotypes (Fig. 5), indicating
 430 that these sequences were only conserved in specific genotypes. The epitope
 431 recognized by mAb clone 3D7 was not in the zinc finger structure of V protein and
 432 was likely not a crucial element for NDV V protein, suggesting it as a potential target
 433 for NDV genotype and subgenotype differentiation.

434

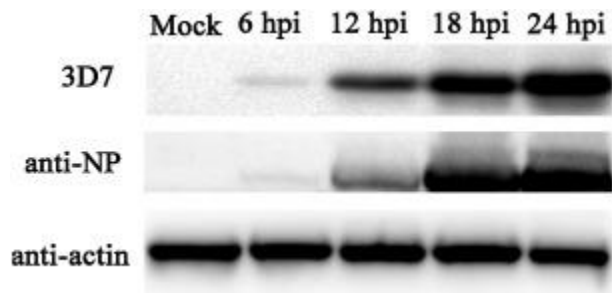
	140	150	160	170
Consensus	E S P G R A S S T S D P T T	G E S A E P R K	Q P G K T A A P G Q G R P	
I AU-0655/99	. P S K K S T K R E . . E H .	
Ulster/67	. P S . A T K S R E . . E	
II PHY-LMV42	. P P . . . S T K S R E . T E	
B1/46	. P . R G E . P . . . S . A T Q S S E . S	
Lasota/46	. P . R G E . P . . . S . A T Q S S E . S	
Beaudette C	. P . R G E P P . . . S . A .	. K . T Q E . S	
II Mukteswar P P A A R .	. . T S . E I . K L	
JS/9/05/Go P P A A R .	. . T S . E I . K L	
JS/7/05/Ch P P A A R .	. . T S . E I . K L	
IV Herts/33 A . A .	. . T S K	
Italian G . A .	. . T S E	
V MX/U.S./Largo/71	K . S R . T . P . . . G Q . .	W W E P I P A	
gamefowl/U.S.(CA)/211472/02	K . S R . T . P . . . G Q . .	W E P I S A	
anhinga/U.S.(Fl)/44083/93	K . S R . T Q A .	W G . . . S W V S E V P A . C R . . .	
VI dove/Italy/2736/00	. P . . G P P . . . G . . .	R . . V . . W R . A . . S C . . .	
IT-227	. P P . . . G . . .	R . . V . . S W R . A . . S	
pi/SH/CH/0167/2013	D P . . G P P . V . G . P .	R W G . A . S . S C . .	
pi/SD/CH/0132/2012	D P . . E P P . . . G . . .	R . . V . . W R . A . S . S C . .	
VII ZJ1	G F . R . . P . . G . . .	R G P . . L W A S	
ch/CN/GX11/2003	G . . R . . P . . G . . .	R . P . . L W A	
JS-3-05-Ch	G . . R . . P I . G . . .	R . P . . L W T A	
JS-5-05-Go	G . S R . . P I . G . . .	R . P . . L W T A	
JSD0812	G . . R . . P . . G . . .	R . P . . L W A S	
VIII QH1	. P T . . I I . V . S	
AF2240 I	W G E A . A . S	
IX JS/1/02/Du N . A .	. . T . . Q S . E . . E	
F48E8 N . A .	. . T . . Q S . E . . E	

435
436

437 *Fig. 5. Alignment of the identified epitope in the V proteins of NDV strains from*
438 *diverse genotypes. V protein sequences from the 27 reference NDV strains of*
439 *different genotypes were from the EMBL/GenBank (Table 1). Prediction of amino*
440 *acid (aa) sequences, alignment of sequences and phylogenetic analysis were*
441 *performed using the MegAlign program in the Lasergene package (DNASTAR Inc.*
442 *Madison, WI, USA). The aa sequence that resembled the consensus sequence is*
443 *indicated by a “.”. The region of the mAb 3D7-recognized peptide*
444 *152RGPAELWK159 identified in the different NDV strains is boxed in the figure.*
445

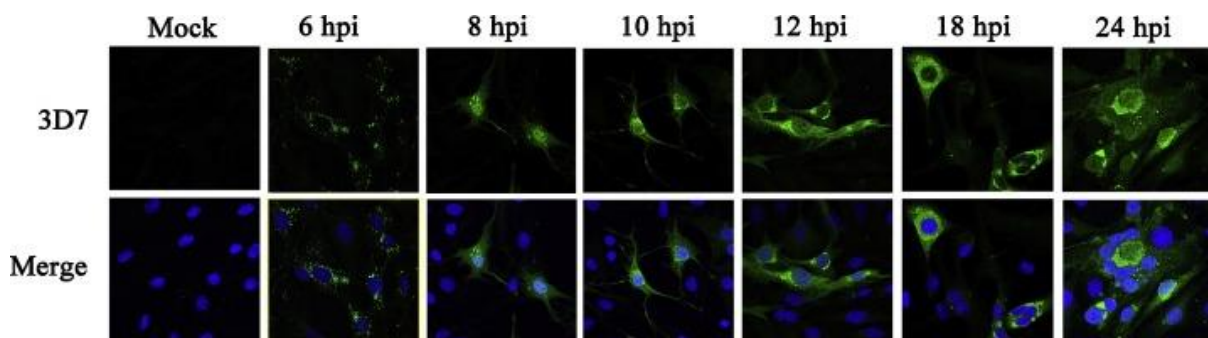
3.7. Expression of V protein during genotype VII NDV infection

446 To determine if mAb clone 3D7 could be used as a tool for immune-detection,
447 dynamic expression of the V protein in NDV-infected cells was surveyed by IFAs and
448 WBs. Firstly, the WB assay of NP protein showed that NDV was propagated in the
449 infected cells. The mAb clone 3D7 reacted with V protein in ZJ-1-infected cells (Fig.
450 6). V protein was detectable at 6 hpi as early as NP of NDV, suggesting it was likely
451 expressed early during the virus's replicative cycle. Similar results were observed by
452 IFAs (Fig. 7). V protein was initially detected at 6 hpi, scattered in the cytoplasm with
453 dotted distribution. From 8 hpi to 12 hpi, V protein accumulated in the cytoplasm and
454 moved towards the periphery of the host cell nucleus. At 18 hpi, some nuclei of
455 infected cells were surrounded by V protein. A large area of syncytia was observed
456 at 24 hpi, and V protein was observed in the middle of the syncytia surrounded by
457 several host nuclei and starting to dissipate.
458
459



460
461
462
463
464
465
466

Fig. 6. Dynamic expression of V protein in DF-1 cells infected with the NDV strain ZJ1 by WB. DF-1 cells were infected with NDV ZJ1 at MOI 5 and collected at 6, 12, 18, 24 hpi. Lysates from cells were immunoblotted with the indicated 3D7, anti-NP and anti-actin monoclonal antibodies.



467
468
469
470
471
472
473
474
475
476

Fig. 7. Dynamic expression of V protein in DF-1 cells infected with the NDV strain ZJ1 by IFA. DF-1 cells were infected with NDV ZJ1 at a MOI of 5 and harvested at 6, 8, 10, 12, 18, 24 hpi. Cells were double stained with the mAb3D7 for V protein and 4',6'-diamidino-2-phenylindole (DAPI) for nuclei. The upper panel of figures show the V protein (green), while the lower figures show overlapping of V protein (green) and DAPI (blue). (For interpretation of the references to colour in this figure legend, the reader is referred to the web version of this article.)

4. Discussion

477
478
479
480
481
482
483
484
485
486
487
488
489
490
491
492
493
494

It has been reported that NDV V protein plays an important role in facilitating virus replication in infected cells via antagonizing cellular IFN signaling (Huang et al., 2003; Park et al., 2003b; Qiu et al., 2016b). The V proteins from distinct NDV strains showed different interferon antagonistic activities (Alamares et al., 2010), albeit the molecular mechanism is unclear since there is little information about the structure and functional domains of NDV V protein. Mapping mAbs binding peptides may shed light on the V protein structure analysis. In this study, a NDV V protein-reactive Mab 3D7 was generated. The reactivity of this mAb was limited to genotype VII strain and could be genotype specific (Fig. 2). To analyze the specificity of mAb 3D7, epitope mapping was performed based on detection of consecutive truncated His-tagged V proteins and synthesized peptides. The results showed that the epitope recognized by mAb 3D7 was located in aa 147–159, and in which peptide 152RGPAELWK159 was essential (Fig. 3).

The epitope (152RGPAELWK159) that we identified in NDV V protein was located at a region after the RNA editing site, which was flanked by two important functional regions, including N-terminal domain of P protein (Karlin et al., 2003; Qiu et al.,

495 2016c) and CTD (Horvath, 2004b); nevertheless, there is rare information regarding
496 this region of NDV V protein at present. Based on the crystal structure of SV5 V
497 protein (Li et al., 2006), the 3D structure of NDV V protein was established using the
498 primary sequence. The predicted 3D structure provides potential useful structural
499 information about the function and antigenic characteristics of the V protein. The
500 predicted V protein structure displayed that the aa 147-159 of V protein was exposed
501 on the protein surface and the core part peptide 152RGPAELWK159 formed a
502 pocket, which would be recognized by the mAb. Furthermore, the reactivity of
503 peptide 152-167 with 3D7 was weaker than peptide 144-159 and 148-163,
504 suggesting that the region of aa 147-151 structurally contributed to epitope
505 presentation on the V protein surface although it was not indispensable for mAb-
506 epitope interaction, which was supported by the 3D structure of V protein.

507

508 One purpose of our study was to determine if V protein could be used as a tool for
509 quick differentiation of genotypes and subgenotypes. Different from their
510 counterparts in other paramyxoviruses, V protein NDVs are reported to be a
511 structural component of virions (Lamb and Kolakofsky, 2002; Steward et al., 1995),
512 which is confirmed by our results (Fig. 2). It suggested that V protein can be used as
513 a detection target for NDV virion. Bioinformatics analysis of the NDV V protein
514 revealed that aa 147-159 of V protein, especially the core peptide
515 152RGPAELWK159 was exposed on the protein surface and displayed strong
516 antigenicity for B-cell recognition based on the online analysis (Table 4), making it a
517 good target epitope for detection.

518

519 The identified and predicted B-cell epitopes were compared (Fig. 5). The identified
520 epitope region aa 147–159 overlapped with predicted epitopes aa 141-148 and aa
521 150-173. Furthermore, the core peptide 152RGPAELWK159 was totally included in
522 the predicted epitopes aa 150-173. Not only linear epitope but the predicted
523 discontinuous epitope aa 141–163 contained all the region recognized by mAb 3D7,
524 suggesting the peptide would contribute to the formation of conformational epitopes.
525 All the above results indicated that the region of NDV V protein recognized by mAb
526 3D7 was highly immunogenic.

527

528 The mAb only react with genotype VII strain and the sequence alignment indicated
529 that the sequence of aa 140-171 of NDV V protein varied among genotypes but was
530 conserved among NDV strains belonging to the same genotype. Importantly, the
531 152RGPAELWK159 was conserved in genotype VII NDV strains, suggesting that the
532 mAb clone 3D7 recognized an epitope specific for genotype VII or VIIId. Defining
533 conserved epitopes can contribute to the development of epitope-based diagnosis
534 methods. It is widely known that most of the prevalent virulent NDV isolates belong
535 to class II, genotype VII; meanwhile, the class I and class II non-virulent strains are
536 spread worldwide due to live vaccine administration and natural infection (Kim et al.,
537 2007; Ramey et al., 2013). The limited genetic and antigenic diversity of NDV
538 genotypes makes quick diagnosis complicated and difficult (Miller et al., 2010). Since
539 the epitope recognized by mAb clone 3D7 was conserved in the genotype VII NDV
540 strains, it could be a potential targeting site for NDV genotype and subgenotype
541 differentiation. However, the NDV isolates used for detection in this study is limited,
542 one cannot rule out the possibility that there would be some NDV variants with
543 different reactivity with 3D7. More detection is required before it can be used for
544 clinical applications. Since the 3D7-recognized region displayed genotype-specific

545 conservation, it can be used as an immunogen to establish more genotype-specific
546 mAbs, or directly used for epitope-based genotype differentiation.

547

548 It is found in this study that the V protein-specific mAb clone 3D7 could be applied to
549 various assays. The expression levels and cellular movement of V protein during
550 viral replication were determined, since the subcellular localization of V protein
551 during NDV replication has not been previously reported. Dynamic expression of V
552 protein in NDV-infected cells was seen in IFAs and WBs (Fig. 6, Fig. 7). Scattering of
553 V protein in the cytoplasm was initially detectable at 6 hpi, and the protein moved to
554 the periphery of the host cell nucleus in the process of infection. At late stage of
555 infection, a mass of V protein was observed around the nuclei of infected cells. This
556 result showed the subcellular movement of NDV V protein in the process of IFN
557 antagonism. In response to NDV infection, latent cytoplasmic STAT proteins are
558 phosphorylated on tyrosine by the Janus family of tyrosine kinase (JAK) enzymes
559 and form a heterotrimer of phosphorylated STAT-1, STAT-2 and IRF-9.
560 Subsequently, this heterotrimer translocates to the nucleus and binds to cis-acting
561 DNA elements to activate the IFN-I-stimulated antiviral genes (Horvath, 2004a, b;
562 Samuel, 2001). V protein has IFN-antagonist activity in the CTD, which promotes
563 degradation of STAT1 and blocks IFN signaling (Alamares et al., 2010; Park et al.,
564 2003b). Our results showed that V protein tend to accumulate around the nuclei of
565 infected cells, suggesting it might act on STAT-1 protein in the course of nuclear
566 import of phosphorylated STAT-1.

567

568 **5. Conclusion**

569 The mAb clone 3D7 against NDV V protein was isolated and the mAb recognized
570 epitope was identified to be 152RGPAELWK159. This peptide was located in a
571 region which was varied in sequence among genotypes but conserved in sequence
572 and structure among NDV strains in the same genotype. The generated V protein-
573 specific mAb clone 3D7 could be applied to various assays and helped us to
574 determine the location of V protein during NDV replication in infected cells. These
575 results extend our understanding of the antigenic structure of V protein and the
576 function of V protein during NDV infection. They also provide a foundation for
577 development of novel, epitope-based genotype differentiation of NDV genotypes.

578

579 **Conflict of interest**

580 The authors declare that they have no competing interests.

581

582 **Author contributions**

583 CD and XQ conceived and designed the research. JL, WW, TR, CM, and YZ
584 performed the experiments. XQ, CM, CS, ZD, XL and YS analyzed the data. LT, SX,
585 WY, XL, VN, MM and YL contributed reagents/materials/analysis tools. XQ and CD
586 wrote the paper.

587

588 **Ethical approval**

589 The Animal experiment protocol was approved by the Institutional Animal Care and
590 Use Committee (IACUC) of Shanghai Veterinary Research Institute (SHVRI),
591 Chinese Academy of Agricultural Sciences (CAAS), and the Permit Number is shvri-
592 mo-0124. The Animal experiment was carried out in agreement with the IACUC
593 guidelines set by SHVRI, CAAS.

594

595 **Informed consent**

596 Informed consent was obtained from all individual participants included in the study.

597

598 **Data availability**

599 All data generated or analyzed during this study are included in this published article.

600

601 **Acknowledgements**

602 This work was funded by the National Key Research and Development Program of
603 China (2016YFD0501603) and Chinese Special Fund for Agro-scientific Research in
604 the Public Interest (201303033).

605

606 **References**

607 J.G. Alamares, S. Elankumaran, S.K. Samal, R.M. Iorio

608 The interferon antagonistic activities of the V proteins from two strains of Newcastle
609 disease virus correlate with their known virulence properties *Virus Res.*, 147 (2010),
610 pp. 153-157

611

612 E.W. Aldous, D.J. Alexander Detection and differentiation of Newcastle disease virus
613 (avian paramyxovirus type 1) *Avian Pathol.*, 30 (2001), pp. 117-128

614

615 A. Czegledi, D. Ujvari, E. Somogyi, E. Wehmann, O. Werner, B. Lomniczi
616 Third genome size category of avian paramyxovirus serotype 1 (Newcastle disease
617 virus) and evolutionary implications
618 *Virus Res.*, 120 (2006), pp. 36-48

619

620 Y. Dai, X. Cheng, M. Liu, X. Shen, J. Li, S. Yu, J. Zou, C. Ding
621 Experimental infection of duck origin virulent Newcastle disease virus strain in ducks
622 *BMC Vet. Res.*, 10 (2014), p. 164

623

624 O. de Leeuw, B. Peeters

625 Complete nucleotide sequence of Newcastle disease virus: evidence for the
626 existence of a new genus within the subfamily Paramyxovirinae
627 *J. Gen. Virol.*, 80 (Pt. 1) (1999), pp. 131-136

628

629

630 L. Didcock, D.F. Young, S. Goodbourn, R.E. Randall

631 The V protein of simian virus 5 inhibits interferon signalling by targeting STAT1 for
632 proteasome-mediated degradation
633 *J. Virol.*, 73 (1999), pp. 9928-9933

634

635

636 D.G. Diel, L.H. da Silva, H. Liu, Z. Wang, P.J. Miller, C.L. Afonso

637 Genetic diversity of avian paramyxovirus type 1: proposal for a unified nomenclature
638 and classification system of Newcastle disease virus genotypes
639 *Infect. Genet. Evol.*, 12 (2012), pp. 1770-1779

640

641 K.M. Dimitrov, A.M. Ramey, X. Qiu, J. Bahl, C.L. Afonso

642 Temporal, geographic, and host distribution of avian paramyxovirus 1 (Newcastle
643 disease virus)

644 *Infect. Genet. Evol.*, 39 (2016), pp. 22-34

645
646 R.E. Gough, D.J. Alexander, M.S. Collins, S.A. Lister, W.J. Cox
647 Routine virus isolation or detection in the diagnosis of diseases in birds
648 Avian Pathol., 17 (1988), pp. 893-907
649
650 A.R. Gould, E. Hansson, K. Selleck, J.A. Kattenbelt, M. Mackenzie, A.J. Della-Porta
651 Newcastle disease virus fusion and haemagglutinin-neuraminidase gene motifs as
652 markers for viral lineage
653 Avian Pathol., 32 (2003), pp. 361-373
654
655 C.M. Horvath
656 Silencing STATs: lessons from paramyxovirus interferon evasion
657 Cytokine Growth Factor Rev., 15 (2004), pp. 117-127
658
659 C.M. Horvath
660 Weapons of STAT destruction. Interferon evasion by paramyxovirus V protein
661 Eur. J. Biochem., 271 (2004), pp. 4621-4628
662
663 Z. Huang, S. Krishnamurthy, A. Panda, S.K. Samal
664 Newcastle disease virus V protein is associated with viral pathogenesis and
665 functions as an alpha interferon antagonist
666 J. Virol., 77 (2003), pp. 8676-8685
667
668 D. Karlin, F. Ferron, B. Canard, S. Longhi
669 Structural disorder and modular organization in Paramyxovirinae N and P
670 J. Gen. Virol., 84 (2003), pp. 3239-3252
671
672 L.M. Kim, D.J. King, D.L. Suarez, C.W. Wong, C.L. Afonso
673 Characterization of class I Newcastle disease virus isolates from Hong Kong live bird
674 markets and detection using real-time reverse transcription-PCR
675 J. Clin. Microbiol., 45 (2007), pp. 1310-1314
676
677 J.V. Kringelum, C. Lundegaard, O. Lund, M. Nielsen
678 Reliable B cell epitope predictions: impacts of method development and improved
679 benchmarking
680 PLoS Comput. Biol., 8 (2012), p. e1002829
681
682 T. Kubota, N. Yokosawa, S. Yokota, N. Fujii
683 C terminal CYS-RICH region of mumps virus structural V protein correlates with
684 block of interferon alpha and gamma signal transduction pathway through decrease
685 of STAT 1-alpha
686 Biochem. Biophys. Res. Commun., 283 (2001), pp. 255-259
687
688 R.A. Lamb, D. Kolakofsky
689 Fundamental virology
690 B.B. Fields, D.M. Kniepe, P.M. Howley (Eds.), Paramyxoviridae: The Viruses and
691 Their Replication, Lippincott Williams & Wilkins, Philadelphia (2002)
692 pp. xi, 1395 p
693
694 T. Li, X. Chen, K.C. Garbutt, P. Zhou, N. Zheng

695 Structure of DDB1 in complex with a paramyxovirus V protein: viral hijack of a
696 propeller cluster in ubiquitin ligase
697 Cell, 124 (2006), pp. 105-117
698

699 X. Liu, X. Wang, S. Wu, S. Hu, Y. Peng, F. Xue
700 Surveillance for avirulent Newcastle disease viruses in domestic ducks (*Anas*
701 *platyrhynchos* and *Cairina moschata*) at live bird markets in Eastern China and
702 characterization of the viruses isolated
703 Avian Pathol., 38 (2009), pp. 377-391
704

705 T. Mebatsion, S. Versteegen, L.T. De Vaan, A. Romer-Oberdorfer, C.C. Schrier
706 A recombinant newcastle disease virus with low-level V protein expression is
707 immunogenic and lacks pathogenicity for chicken embryos
708 J. Virol., 75 (2001), pp. 420-428
709

710 L. Mia Kim, D.J. King, D.L. Suarez, C.W. Wong, C.L. Afonso
711 Characterization of class I Newcastle disease virus isolates from Hong Kong live bird
712 markets and detection using real-time reverse transcription-PCR
713 J. Clin. Microbiol., 45 (2007), pp. 1310-1314
714
715

716 P.J. Miller, E.L. Decanini, C.L. Afonso
717 Newcastle disease: evolution of genotypes and the related diagnostic challenges
718 Infect. Genet. Evol., 10 (2010), pp. 26-35
719

720 H. Palosaari, J.P. Parisien, J.J. Rodriguez, C.M. Ulane, C.M. Horvath
721 STAT protein interference and suppression of cytokine signal transduction by
722 measles virus V protein
723 J. Virol., 77 (2003), pp. 7635-7644
724
725

726 M.S. Park, A. Garcia-Sastre, J.F. Cros, C.F. Basler, P. Palese
727 Newcastle disease virus V protein is a determinant of host range restriction
728 J. Virol., 77 (2003), pp. 9522-9532
729

730 M.S. Park, M.L. Shaw, J. Munoz-Jordan, J.F. Cros, T. Nakaya, N. Bouvier, P.
731 Palese, A. Garcia-Sastre, C.F. Basler
732 Newcastle disease virus (NDV)-based assay demonstrates interferon-antagonist
733 activity for the NDV V protein and the Nipah virus V, W, and C proteins
734 J. Virol., 77 (2003), pp. 1501-1511
735
736

737 R.G. Paterson, G.P. Leser, M.A. Shaughnessy, R.A. Lamb
738 The paramyxovirus SV5 V protein binds two atoms of zinc and is a structural
739 component of virions
740 Virology, 208 (1995), pp. 121-131
741

742 X. Qiu, Q. Sun, S. Wu, L. Dong, S. Hu, C. Meng, Y. Wu, X. Liu
743 Entire genome sequence analysis of genotype IX Newcastle disease viruses reveals
744 their early-genotype phylogenetic position and recent-genotype genome size

745 Virol. J., 8 (2011), p. 117
746
747
748 X. Qiu, Q. Fu, C. Meng, S. Yu, Y. Zhan, L. Dong, T. Ren, Y. Sun, L. Tan, C. Song, X.
749 Han, C. Ding
750 Kinetic analysis of RNA editing of Newcastle disease virus P gene in the early period
751 of infection
752 Acta Virol., 60 (2016), pp. 71-77
753
754
755 X. Qiu, Q. Fu, C. Meng, S. Yu, Y. Zhan, L. Dong, C. Song, Y. Sun, L. Tan, S. Hu, X.
756 Wang, X. Liu, D. Peng, X. Liu, C. Ding
757 Newcastle disease virus V protein targets phosphorylated STAT1 to block IFN-I
758 signaling
759 PloS one, 11 (2016), p. e0148560
760
761 X. Qiu, Y. Zhan, C. Meng, J. Wang, L. Dong, Y. Sun, L. Tan, C. Song, S. Yu, C. Ding
762 Identification and functional analysis of phosphorylation in Newcastle disease virus
763 phosphoprotein
764 Arch. Virol, 161 (2016), pp. 2103-2116
765
766